International Conference on Mathematics and Computational Methods Applied to Nuclear Science and Engineering (M&C 2011)
Rio de Janeiro, RJ, Brazil, May 8-12, 2011, on CD-ROM, Latin American Section (LAS) / American Nuclear Society (ANS)
ISBN 978-85-63688-00-2

TECHNIQUES TO REDUCE MEMORY REQUIREMENTS FOR COUPLED PHOTON-ELECTRON TRANSPORT

Bruno Turcksin, Jean Ragusa, and Jim Morel
Texas A&M University, Department of Nuclear Engineering
College Sation, Texas 77843-3133
turcksin@neo.tamu.edu; ragusa@ne.tamu.edu; morel@ne.tamu.edu

ABSTRACT

In this work, we present two methods to decrease memory needs while solving the photon-electron transport equation. The coupled transport of electrons and photons is of importance in radiotherapy because it describes the interactions of X-rays with matter. One of the issues of discretized electron transport is that the electron scattering is highly forward peaked. A common approximation is to represent the peak in the scattering cross section by a Dirac distribution. This is convenient, but the integration over all angles of this distribution requires the use of Galerkin quadratures. By construction these quadratures impose that the number of flux moments be equal to the number of directions (number of angular fluxes), which is very demanding in terms of memory. In this study, we show that even if the number of moments is not as large as the number of directions, an accurate solution can be obtained when using Galerkin quadratures. Another method to decrease the memory needs involves choosing an appropriate reordering of the energy groups. We show in this paper that an appropriate alternation of photons/electrons groups allows us to rewrite one transport problem of n groups as gcd successive transport problems of $\frac{n}{gcd}$ groups where gcd is the greatest common divisor between the number of photon groups and the number of electron groups.

Key Words: Galerkin quadrature, photon-electron transport, radiotherapy

1. INTRODUCTION

The transport of photons and electrons has many applications in medical physics and particularly in radiotherapy. Radiotherapy uses photons and charged particles to damage the DNA of cancerous cells. While using photons, free electrons are created; this ionizes the environment and creates free radicals that damage the cells DNA. One quantity used to gauge whether a cell will die due to radiation is the absorbed dose, defined as the energy deposited per unit of mass and measured in Gray $\left(Gy = \frac{J}{kg}\right)$. Several methods can be applied to solve the photon-electron distribution in the body : semi-analytic methods, deterministic methods and Monte-Carlo methods. Monte-Carlo methods yield very accurate results, however they are slow to converge and thus, remain too slow for effective clinical use [1]. Other methods, such as pencil-beam convolution and convolution-superposition, employ pre-calculated Monte-Carlo dose kernels, which are then locally scaled to approximate photon and electron transport in the presence of heterogeneities. These methods present some issues in the presence of large density gradients, such as those found at interfaces between different materials: air, bone, lung and soft tissue [1–3]. If

enough cells are used, deterministic methods can be accurate even on interfaces between materials [1]. These methods are faster than Monte-Carlo methods but slower than the semi-analytic methods.

In this work, we present a S_n method for photon-electron transport. The difficulty of this calculation comes from the transport of the electrons. Because the electrons are charged particles, they have highly anisotropic scattering due to their interactions with other particles through Coulomb interaction. This anisotropy causes some complications since the standard Legendre expansion representing the cross sections would require hundreds of terms. A common approximation is to use a Dirac distribution to model the forward-peaked scattering of the electrons and a continuous slowing down term for energy loss due to Coulomb interactions. This allows the Legendre expansion of the cross section to be kept to a low order. However, an exact integration of the Dirac distribution requires the use of Galerkin quadratures [4] that demand a significant amount of memory. These quadratures require the number of flux moments and the number of angular fluxes to be equal and this number varies, for triangular quadratures, as $\frac{n(n+2)}{8}$ per octant with the order of the S_n method. For example, when using the S_n discretization for $n = 16$, we have, in 3D, 288 directions and thus, 288 angular fluxes or flux moments to store.

In this work, we analyze the effects of truncation on the Galerkin quadratures. To do this, we alter the order of the scattering cross sections and observe the effect on the absorbed dose. The goal is to keep as few flux moments as possible while maintaining an accurate solution.

We also show a method of ordering the energy groups which allows us the decomposition one large transport problem into several smaller transport problems. We can do this because there is no thermalization of the particles. Therefore, every particle undergoes only slowing down and the scattering matrix can be written as a lower block triangular matrix. The interactions between photons and electrons forbid a lower triangular matrix by adding some upscattering terms in the scattering matrix. The code generating the cross sections, CEPXS [5], generates first the cross sections for one particle type and then, the cross sections for the other one. We show in this paper how to improve the order of the groups.

2. EQUATIONS

In this section, we present the equation that models the transport of electrons. We will also show why it is so important to use Galerkin quadratures. First, we present the Boltzmann-Fokker-Planck equation (BFP). The idea is to decompose the highly forward peaked scattering cross section into a sum of a forward-peaked cross section and a smoothly varying cross section. The BFP equation is given by (the variables are omitted for brevity) [6] :

$$\begin{aligned}\boldsymbol{\Omega}\cdot\boldsymbol{\nabla}\Psi+\Sigma_t\Psi=&\int_{4\pi}\int_0^\infty\Sigma_s\left(\boldsymbol{\Omega}\cdot\boldsymbol{\Omega}',E'\rightarrow E\right)\Psi(\boldsymbol{\Omega}',E')dE'd\boldsymbol{\Omega}'\\&+\frac{\alpha}{2}\left(\frac{\partial}{\partial\mu}\left(1-\mu^2\right)\frac{\partial\Psi}{\partial\mu}+\frac{1}{1-\mu^2}\frac{\partial^2\Psi}{\partial\phi^2}\right)+\frac{\partial S\Psi}{\partial E}+Q\end{aligned}\tag{1}$$

where :

- Ψ is the angular flux
- Σ_t is the smooth-component of the total macroscopic cross section

- Σ_s is the smooth-component of the macroscopic differential scattering cross section
- Q is a volumetric source
- μ is the cosine of the directional polar angle
- ϕ is the directional azimuthal angle

The second and the third term of the right-hand-side change the direction of the particles without changing their energy and the fourth term changes the energy of the particles without changing their direction (continuous slowing-down term) [7]. The continuous slowing down is used for the "soft" interactions that result in small-energy losses. The catastrophic interactions that result in large energy losses are represented with the standard Boltzmann operator. α is the restricted momentum transfer :

$$\alpha(E) = 2\pi \int_0^E \int_{-1}^1 \Sigma_{ss}(E \to E', \mu_0)(1-\mu_0) d\mu_0 dE' \ , \tag{2}$$

with $\mu_0 = \mu'\mu + \sqrt{(1-\mu'^2)\,(1-\mu^2)} cos\,(\phi' - \phi)$ and $\Sigma_{ss}(E \to E', \mu_0)$ denotes the forward-peaked scattering cross section.
S is the restricted stopping power :

$$S(E) = 2\pi \int_0^E \int_{-1}^1 \Sigma_{ss}(E \to E', \mu_0) \left(E - E'\right) d\mu_0 dE' \ . \tag{3}$$

The restricted stopping power is defined as the portion of the total stopping power that is not due to catastrophic collisions.
Standard boundary conditions can be applied to (1), the most likely being the vacuum boundary conditions :

$$\Psi(\mathbf{r}, \mathbf{\Omega}, E) = 0 \quad \text{for } \mathbf{\Omega} \cdot \boldsymbol{n} < 0 \text{ and } \mathbf{r} \in \partial\mathcal{D}_v \tag{4}$$

and the incoming flux boundary conditions :

$$\Psi(\mathbf{r}, \mathbf{\Omega}, E) = g(\mathbf{r}, \mathbf{\Omega}, E) \quad \text{for } \mathbf{\Omega} \cdot \boldsymbol{n} < 0 \text{ and } \mathbf{r} \in \partial\mathcal{D}_i \ , \tag{5}$$

where $\partial\mathcal{D}_v$ is the boundary of the domain where vacuum conditions are applied and $\partial\mathcal{D}_i$ is the boundary of the domain where incoming flux conditions are applied.
In this work, we will use another approach and retain only the asymptotic limit on the energy dependence but not the angular dependence. We will keep the continuous slowing-down term and approximate the forward peaked angular dependence by a Dirac distribution. The equation can be written as :

$$\begin{aligned} \mathbf{\Omega} \cdot \boldsymbol{\nabla}\Psi + \Sigma_t \Psi = & \int_{4\pi} \int_0^\infty \Sigma_s \left(\mathbf{\Omega} \cdot \mathbf{\Omega}', E' \to E\right) \Psi(\mathbf{\Omega}', E') dE' d\mathbf{\Omega}' \\ & + \int_{-1}^1 c\delta(\mu - 1)\Psi d\mu + \frac{\partial S\Psi}{\partial E} + Q \ . \end{aligned} \tag{6}$$

The continuous slowing-down term in the equation (6) can be either treated explicitly or it can be treated in the cross sections. The latter was done in the CEPXS code which produces cross sections for photons and electrons transport [5]. In this work, we use cross sections produced

by CEPXS to compute the coupled photon-electron transport. Unlike [1], we do not assume that the electrons do not produce photons. The system is fully coupled, meaning that photons produce electrons and electrons produce photons. Thus, there are upscattering terms present in the scattering matrix even if there is not upscattering physically. The upscattering is between particle types; a given particle can only lose energy and create others particle types that are represented by the upscattering terms.
Next, we focus on the scattering term, assuming that this quantity has been integrated over the energy range :

$$R = \int_{4\pi} \Sigma_s \left(\mathbf{\Omega} \cdot \mathbf{\Omega}'\right) \Psi \left(\mathbf{\Omega}'\right) d\mathbf{\Omega}' + \int_{-1}^{1} c\delta(\mu - 1)\Psi d\mu \tag{7}$$

In a S_n code, it is usual to write the discretized scattering source (7) as a product of three matrices [4] :

$$\boldsymbol{R} = M\Sigma D\boldsymbol{\Psi} \tag{8}$$

where $\boldsymbol{R}$ is the vector containing the scattering source, $\boldsymbol{\Psi}$ is the vector containing all the flux moments, D is the discrete-to-moment matrix which maps a vector of discrete angular flux values to a corresponding vector of flux moments, Σ is the scattering matrix which contains the moments of the scattering cross sections on its diagonal, and M is the moment-to-discrete matrix which maps a vector of flux moments to a corresponding vector of discrete angular flux values. The Galerkin quadratures require that :

$$D = M^{-1} \tag{9}$$

and, therefore, M and D have to be square matrices. This implies that the number of moments is equal to the number of directions.
Galerkin quadratures exactly integrate a delta function scattering cross-sections. If we assume :

$$\Sigma(\mu) = \delta(\mu - 1) \ , \tag{10}$$

We see that :

$$\begin{aligned} R &= \int_{-1}^{1} \delta(\mu - 1)\Psi(\mu)d\mu \\ &= \Psi \end{aligned} \tag{11}$$

Because $P_l(1) = 1$ for all l, all expansion coefficients for the delta function are equal to unity, and the cross-section matrix is the identity matrix. We get :

$$\boldsymbol{R} = MD\boldsymbol{\Psi} = \boldsymbol{\Psi} \ . \tag{12}$$

3. MEMORY ISSUES

In the previous section, we showed that one should employ a Galerkin quadrature to solve (6) correctly. This may be a significant issue in terms of memory requirements. For neutron transport, the scattering is less anisotropic than for electron transport, and therefore, fewer flux moments than angular fluxes are needed. This is the reason why the information is usually stored as flux moments. However, Galerkin quadratures require the number of moments to be equal to the number of directions. This requirement is very restrictive and it is important to

explore whether it is possible to decrease the number of moments while maintaining a larger number of directions. In [8], the authors used a Legendre expansion of the scattering cross section with an order lower than that required by the Galerkin quadrature. They have shown a good agreement between their results and Monte-Carlo simulations. In the next section, we study the effects of truncating the Legendre expansion while keeping a larger number of angular fluxes than the order of the scattering expansion. We proceed by building the matrices M and D using a Galerkin quadrature, then truncate them to keep only a few moments. Therefore, M and D are rectangular instead of square matrices and a truncated scattering expansion can be used. We show the results for two materials, Al and Au, and for different Legendre expansions.

4. RESULTS

In this section, we compare our results using PDT with those computed using ONELD[5]. PDT is a three dimensional Parallel Deterministic Transport code developed at Texas A&M University while ONELD is a code that solves the equation (6) in one dimension using the cross sections generated by CEPXS. ONELD always uses the full scattering order to solve photon-electron transport problems. To compare the results produced by the two codes, we use equivalent angular discretization, Gauss-Legendre for ONELD, and Gauss-Legendre-Chebyshev (GLC) for our code. The GLC quadrature consists of a Gauss-Legendre quadrature for the polar angle and a Chebyshev quadrature for the azimuthal angle. The n-points Chebyshev quadrature uses n points equally spaced between 0 and 2π. When the solution is independent of the azimuthal angle, the GLC quadrature is equivalent to the one dimensional Gauss-Legendre quadrature. The results of ONELD gives only the average dose on a cell while the results of our code gives the dose at a given point. To compare the dose at any given point, we interpolate the values given by ONELD.

4.1 Aluminium

The medium is 5 cm thick and made of aluminium. We use a S_{12} quadrature. There is an incoming flux of photons of 1 $\frac{photon}{cm^2}$. The direction of the incoming flux is chosen to be the most normal direction of the quadrature. The source of photons has an energy of 20 MeV and we use a cut-off energy of 0.01 MeV. Every particle that has an energy lower than 0.01 MeV is assumed to deposit all its energy without moving further.
In the following table, we vary the number of moments and we show the dose computed every centimeter using different scattering orders. Notice that the order thirteen is the full order, i.e. the number of moments equals the number of directions.

Table I: Dose in $\frac{MeV}{g}$ for different scattering orders

Position (cm)	ONELD	PDT				
		order = 13	order = 11	order = 9	order = 7	order = 5
0	0.015003	0.0146404	0.0146402	0.0141156	0.0166718	0.0087276
1	0.169908	0.1697907	0.1697890	0.1698012	0.1695422	0.1728969
2	0.275425	0.2752749	0.2752729	0.2753298	0.2742052	0.2775113
3	0.316307	0.3161310	0.3161307	0.3165279	0.3145572	0.3199176
4	0.312283	0.3120572	0.3120566	0.3125514	0.3104412	0.3153226
5	0.233048	0.2087631	0.2087634	0.2094064	0.2061794	0.2154810

The relative error are :

Table II: Relative error in percentage for different scattering orders

Position (cm)	PDT				
	order = 13	order = 11	order = 9	order = 7	order = 5
0	2.41%	2.41%	5.91%	11.1%	41.8%
1	0.069%	0.07%	0.062%	0.21%	1.79%
2	0.054%	0.055%	0.035%	0.44%	0.76%
3	0.056%	0.056%	0.070%	0.55%	1.14%
4	0.072%	0.072%	0.085%	0.59%	0.97%
5	10.42%	10.42%	10.14%	11.53%	7.53%

The agreement between ONELD and our code using the full order is excellent. The differences on the edges of the domain are larger, due to the fact that the dose varies quickly near the border. Because of this, the interpolation used to find the value at a given point by ONELD is less precise.
We see that if we discard the results on the edges of the domain, the results obtained by using a P_5 order for the scattering are very close to the ones using the full order in the scattering cross-section expansion. The reason is that the high order flux moments are very small compared to the low order flux moments (see Figure 1 to Figure 6). In the following figures, the abscissa is the distance in centimeters and the ordinate is the value of the flux in $\frac{particles}{cm^2 s}$.

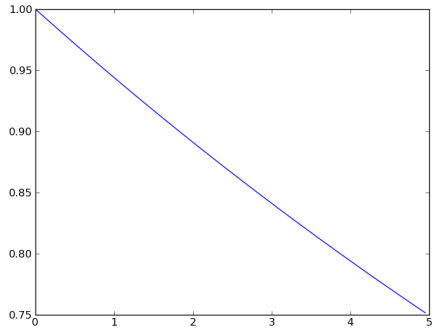

Figure 1: Scalar flux in the first photon group

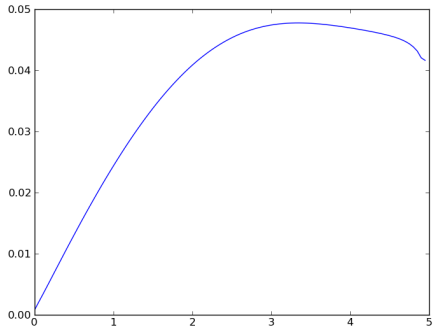

Figure 2: Scalar flux in the last electron group

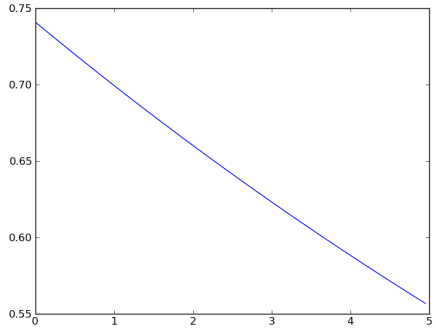

Figure 3: Moment P_5^0 of the flux in the first photon group

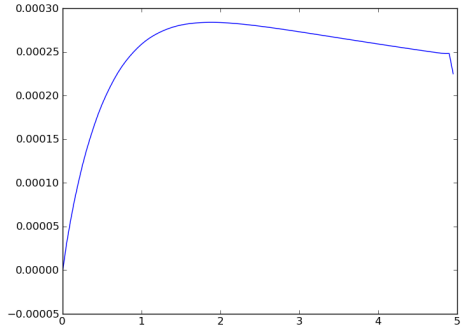

Figure 4: Moment P_5^0 of the flux in the last electron group

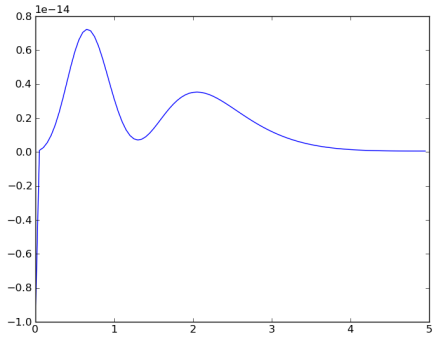

Figure 5: Moment P_{11}^0 of the flux in the first photon group

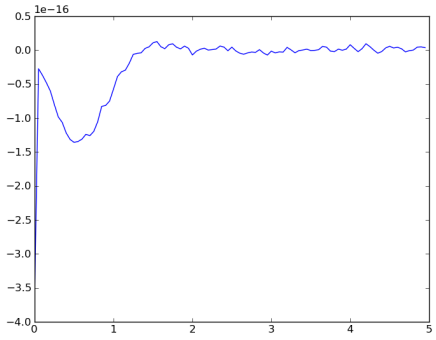

Figure 6: Moment P_{11}^0 of the flux in the last electron group

4.2 Gold

The setup of this problem is the same as for the previous simulations but the medium considered here is gold. In the next table, we provide the dose computed every centimeter using different scattering orders :

Table III: Dose in $\frac{\text{MeV}}{\text{g}}$ for different scattering orders

Position (cm)	ONELD	PDT			
		order = 11	order = 9	order = 7	order = 5
0	0.11675	0.097168	0.097155	0.097073	0.097326
1	0.41799	0.420905	0.420871	0.420988	0.421102
2	0.16284	0.164953	0.164946	0.165017	0.164605
3	0.06407	0.065297	0.065300	0.065292	0.065214
4	0.02566	0.026303	0.026304	0.026295	0.026318
5	0.00847	0.006082	0.006083	0.006075	0.006112

The relative errors are given in the next table :

Table IV: Relative error in percentage for different scattering orders

Position (cm)	PDT			
	order = 11	order = 9	order = 7	order = 5
0	16.77%	16.78%	16.85%	16.64%
1	0.70%	0.70%	0.72%	0.74%
2	1.30%	1.29%	1.02%	1.08%
3	1.92%	1.92%	1.91%	1.79%
4	2.51%	2.51%	2.47%	2.56%
5	28.19%	28.18%	28.28%	27.84%

We can see that there is no need to use the full order to solve the problem. The differences between the order five and order eleven are small. For this reason, we expect the results of the order eleven to be very close from the ones of order eleven. The difference between the order eleven and ONELD is about 2% in the middle of the domain while the difference is larger on the boundary of the domain due to the interpolation of the ONELD results.

5. REORDERING

The second method to decrease memory required to solve the transport of photons-electrons involves reordering the energy groups to simplify the scattering cross-section matrix. When CEPXS generates the cross sections, it first writes all the cross sections for one particle type, and then, the cross sections for the other particle type into the scattering matrix. The energy

range is the same for the two particles. The cross section matrix looks like :

$$\Sigma = \begin{pmatrix} PP & EP \\ PE & EE \end{pmatrix} \tag{13}$$

where PP and EE are lower triangular matrices which represent the scattering for each particle type. The two matrices are lower triangular because only down scattering is allowed. The cut-off energy used in radiotherapy approximations forbids the thermalization of particles. Matrix EP represents the creation of photons by electrons through bremsstrahlung production and fluorescence production. Matrix PE represents the creation of electrons by photons through photoelectric effect, Compton scattering, pair electron production, and Auger production following photoionization. Now it is important to notice that because of energy conservation, a particle can only create a particle which has a energy equal or lower than its own. An example of the transfer of two photon groups and four electron groups can be seen in Figure 7 :

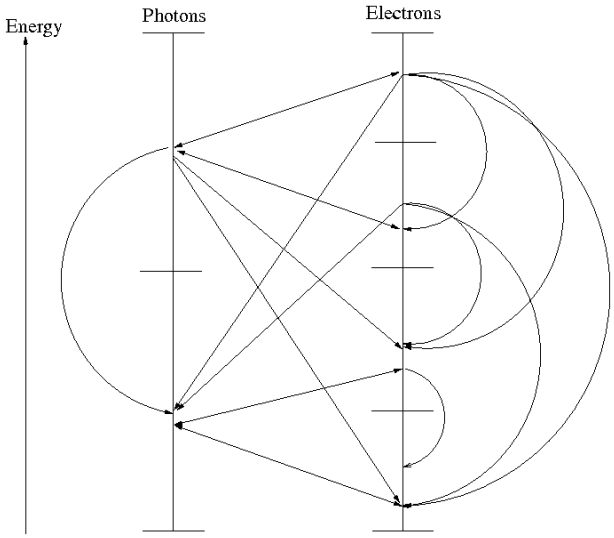

Figure 7: Transfer between the different groups

The pattern of the scattering matrix is as follows :

$$\Sigma = \left(\begin{array}{cc|cccc} x & 0 & x & x & 0 & 0 \\ x & x & x & x & x & x \\ \hline x & 0 & x & 0 & 0 & 0 \\ x & 0 & x & x & 0 & 0 \\ x & x & x & x & x & 0 \\ x & x & x & x & x & x \end{array}\right) \tag{14}$$

We can see that there is no upscattering to the first group of photons, the first and the second group of electrons coming from the second group of photons, and the third or the fourth group of electrons (see Figure 7). If we reorder the groups using for the first group set : photon group 1, electron group 1, electron group 2 and for the second group set : photon group 2, electron

group 3, electron group 4. The pattern of the scattering matrix looks like :

$$\Sigma = \left(\begin{array}{ccc|ccc} x & x & x & 0 & 0 & 0 \\ x & x & 0 & 0 & 0 & 0 \\ x & x & x & 0 & 0 & 0 \\ \hline x & x & x & x & x & x \\ x & x & x & x & x & 0 \\ x & x & x & x & x & x \end{array}\right) \tag{15}$$

Now, we see that the matrix is block lower triangular and we can solve the transport problem by solving two problems with only three groups each. We can solve the first three groups without solving the last three groups since there is no upscattering coming from these. Then, we can solve the last three groups, with the first three groups hidden in the source term. If there are more than two group sets, the fixed source, which now contains the scattering source, can be saved on an auxiliary memory, like for example on the hard disk. Only the source for the groups of the group set that we are solving are needed in memory. To know how many groups we need to gather from each particle in each group set, we can use a simple rule. First, we define the number of photon groups as n_p, the number of electron groups as n_e and the greatest common divisor between these two numbers as *gcd*. The number of photon groups to put in a group set is $\frac{n_p}{gcd}$ and the number of electron groups to put in a group set is $\frac{n_e}{gcd}$. Instead of solving one problem of n groups, we can solve *gcd* problems of $\frac{n}{gcd}$ groups. Notice that we assumed that CEPXS generates groups of equal energy per groups. This is only one of the two ways used by CEPXS to generate the cross sections. For the other one, the energy per group varies logarithmically. In this case, if we assume that $n_e \geq n_p$, we will have n_p group sets, $n_p - 1$ group sets containing each one electron group and one photon group and one group containing the photon group of lowest energy and the $n_e - (n_p - 1)$ electron groups of lowest energy.
Reordering the groups can also decrease the number of source iteration or GMRES iterations. These two methods are used to solve the linear system created by the discretized transport equation of (6). Below, we compare the number of iterations needed to solve a problem similar to the one described in the previous section with and without reordering. The domain is made of aluminium, we use a S_{12} angular discretization and P_5 expansion for the scattering cross section. We use linear discontinuous finite elements for the spatial discretization. The range of energy studied is [0.01MeV,10MeV]. There are 180 cells and we have 15 groups of photon and 25 groups of electron. We compare three methods : the standard multigroup iterative scheme, the standard multigroup iterative scheme with reordering and the blocked multigroup iterative scheme. The last scheme solves eight multigroup transport problems, each of them having only five groups. We obtain the following result :

Table V: Comparison of the number of iterations with and without group reordering

	With reordering		Without reordering
	Modified multigroup	Standard multigroup	Standard multigroup
Total inner iterations	4232	6956	7398
Total outer iterations	$17 \approx 2$ per block	5	5

Reordering the groups decreases the number of inner iterations by 6% while the blocked scheme reduces the number of inner iterations by 42% compare to the standard multigroup scheme.

6. CONCLUSIONS

In this paper, we have shown that it is not necessary to keep the full order of the scattering cross sections to obtain an accurate result while solving photon-electron transport. Truncating the Galerkin quadrature or equivalently truncating the scattering expansion while keeping a large number of directions allows us to significantly decrease the memory requirements. We also presented a method to advantageously reorder the energy groups in the scattering matrix. The groups can be reordered in such a way that a problem with n_p groups of photons and n_e groups of electrons can be rewritten as *gcd* problems of $\frac{n_p+n_e}{gcd}$ groups, where *gcd* is the greatest common divisor between n_p and n_e. The reordering also decreases the number of iterations needed to solve the multigroup transport equation. These two methods can significantly decrease the memory needed to solve coupled photon/electron transport problems.

REFERENCES

1. Oleg N. Vassiliev, Todd A. Wareing, John McGhee, Gregory Failla, Mohammad R. Salehpour, and Firas Mourtada. Validation of a new grid-based Boltzmann equation solver for dose calculation in radiotherapy with photo beams. *Physics in Medicine and Biology*, 55, 2010.

2. J. Seco, E. Adams, M. Bidmead, M. Partridge, and F. Verhaegen. Head-and-neck IMRT treatments assessed with a Monte-Carlo dose calculation engine. *Physics in Medicine and Biology*, 50, 2005.

3. Thomas Krieger and Otto A Sauer. Monte-Carlo- versus pencil-beam-/collapsed-cone-dose calculation in a heterogeneous multi-layer phantom. *Physics in Medicine and Biology*, 50, 2005.

4. J. E. Morel. A Hybrid Collocation-Galerkin-Sn Method for Solving the Boltzmann Transport Equation. *Nuclear Science and Engineering*, 101, 1989.

5. CEPXS/ONELD 1.0 manual user. *RSICC Computer Code Collection.*

6. J.E. Morel and D.P. Sloan. A Hybrid Multigroup/Continuous-Energy Monte-Carlo Method for Solving the Boltzmann-Fokker-Planck Equation. *Nuclear Science and Engineering*, 124, 1996.

7. J.E. Morel. Fokker-Planck Calculations Using Standard Discrete Ordinates Transport Codes. *Nuclear Science and Engineering*, 79, 1981.

8. Kent A. Gifford, John L. Horton Jr., Todd A. Wareing, and Gregory Failla Firas Mourtada. Comparison of a finite-element multigroup discrete-ordinates codes with Monte-Carlo for radiotherapy calculations. *Physics in Medicine and Biology*, 51, 2006.